Journal of Nonlinear Mathematical Physics Volume 15, Supplement 3 (2008), 53–64 ARTICLE

The Motion of a Gyrostat in a Central Gravitational Field: Phase Portraits of an Integrable Case

M C Balsas [a], E S Jiménez [a] and J A Vera [b]

[a] *Consejería de Educación y Cultura, Comunidad Autónoma de la Región de Murcia, Spain*
[b] *Departamento de Matemática Aplicada y Estadística, Universidad Politécnica de Cartagena, C/ Doctor Fleming s/n, 30202, Cartagena (Murcia), Spain*
E-mail: juanantonio.vera@upct.es

Abstract

In this paper we describe the Hamiltonian dynamics, in some invariant manifolds of the motion of a gyrostat in Newtonian interaction with a spherical rigid body. Considering a first integrable approximation of this roto-translatory problem, by means of Liouville-Arnold theorem and some specifics techniques, we obtained a complete topological classification of the phase flow associated to this system. The action-angle variables regions are obtained. These variables allow us to calculate the modified Keplerian elements of this problem useful to elaborate a perturbation theory. The results of this work have a direct application to the study of two body roto-translatory pro-blems where the rotation of one of them influences strongly in the orbital motion of the system. In particular, we can apply these results to binary asteroids.

1 Introduction

In this work we describe the qualitative analysis of the dynamics of a first integrable approximation of a gyrostat in Newtonian interaction with a spherical rigid body, in the fibers of constant total angular momentum vector of an invariant manifold of motion. Let us remember what is known as gyrostat: a mechanical system S composed of a rigid body S' and other bodies S'' (deformable or rigid) connected to it, in such a way that their motion relative to S' does not alter the distribution of masses of the system S. Examples of such systems are: a rigid body to which are connected axes of several symmetric rotors; or a rigid body with cavities completely filled with a homogeneous fluid (see [9], [5], [3] for details).

As in [8], in some invariant manifolds of the motion, the dynamics of the non-canonical hamiltonian system is described, in a first approximation of the gravitational potential, by the Hamiltonian $\mathscr{H} : \mathbf{E} \longrightarrow \mathbb{R}$ given by:

$$\mathscr{H} = \mathscr{H}_{Kepler} + \alpha(\beta - p_\theta)^2 \tag{1.1}$$

where $\mathscr{H}_{Kepler}$ represents the Kepler Hamiltonian associated to the classical two-body problem and $\alpha(\beta - p_\theta)^2$ is the effect associated to the rotation of the gyrostat. Where $\alpha > 0$ and $\beta \in \mathbb{R}$ are two structural constants of the system and $\mathbf{E} = \mathbb{R}^+ \times S^1 \times \mathbb{R}^2$ is the phase space.

In order to do a qualitative study of the dynamics associated to the Hamiltonian system, in a similar way to [4], we consider the following sets:

$$I_h = \mathscr{H}^{-1}(h) = \{z \in \mathbf{E} : \mathscr{H}(z) = h\}, \quad I_k = \{z \in \mathbf{E} : p_\theta = k\} \quad \text{and} \quad I_{hk} = I_h \cap I_k$$

with $z = (r, \theta, p_r, p_\theta) \in \mathbf{E}$ and $(h,k) \in \mathbb{R}^2$.

These sets are invariant by the flow associated to the Hamiltonian, being $\mathscr{H}$ and p_θ two first integrals of motion, independent and in involution.

The main results of this paper are the description of the foliation of:

(a) The phase space $\mathbf{E}$ by the invariant sets I_h.

(b) I_h by the invariant sets I_{hk}.

(c) I_{hk} by the flow of the Hamiltonian system.

This foliation provides a good description of the phase space when $(h,k) \in \mathbb{R}^2$ varies for different values of α and β.

The main tool for this study is the Liouville-Arnold theorem ([1],[4]), applied to the momentum map $(\mathscr{H}, p_\theta) : \mathbf{E} \times \mathbb{R} \longrightarrow \mathbb{R}^2$ at regular values. A particular study for the sets I_h, I_k and I_{hk} for critical values of the momentum map is made. These values come given by the equilibrium points of $\mathscr{H}$ or by values where $p_\theta = k$ is a maximum or a minimum of the energy surface.

In order to conclude we obtain the action-angle variables and the region of the phase space where they can be defined. We calculate the Delaunay variables and the modified Keplerian elements of this problem useful to elaborate a perturbation theory.

2 Hamiltonian dynamics of the system

2.1 Equations of motion

According to [8], we use the following notation: S_0 is a gyrostat of mass m_0 and S_1 is a spherical rigid body of mass m_1. $M_1 = m_0 + m_1$; $g_1 = m_0 m_1 / M_1$; $\mathbf{u}$, $\mathbf{v}$ vectors of $\mathbb{R}^3$; $\mathbf{I}_{\mathbb{R}^3}$ is the identity matrix and $\mathbf{0}$ is the zero matrix of order three; $\mathbb{I} = diag(A,B,C)$ the diagonal tensor of inertia of the gyrostat, $\mathbf{z} = (\Pi, \mathbf{u}_1, \mathbf{p}_1) \in \mathbb{R}^9$ is a generic element of the twice reduced problem obtained using the symmetries of the system; $\Pi = \mathbb{I}\Omega + \mathbf{l}_r$ is the total rotational angular momentum vector of the gyrostat in the body frame, which is attached to its rigid part $\mathfrak{J}$ and whose axes have the direction of the principal axes of inertia of S_0; $\mathbf{l}_r = (0,0,l)$ is the gyrostatic momentum due to the relative motion in the gyrostat, that we assume constant and parallel to the third axis of inertia; $\mathbf{u}_1, \mathbf{p}_1$ are the barycentric coordinates and linear momenta expressed in the body frame $\mathfrak{J}$ and $\mathbf{L} = \Pi + \mathbf{u_1} \times \mathbf{p_1}$.

Let $\mathbf{M} = \mathbb{R}^9$ and we consider the following Lie-Poisson system $(\mathbf{M}, \{\ ,\ \}, \mathscr{H})$, with Poisson brackets $\{\ ,\ \}$ defined by means of the Poisson tensor:

$$\mathbf{B}(\mathbf{z}) = \begin{pmatrix} \widehat{\Pi} & \widehat{\mathbf{u}_1} & \widehat{\mathbf{p}_1} \\ \widehat{\mathbf{u}_1} & \mathbf{0} & I_{\mathbb{R}^3} \\ \widehat{\mathbf{p}_1} & -I_{\mathbb{R}^3} & \mathbf{0} \end{pmatrix} \tag{2.1}$$

In $\mathbf{B}(\mathbf{z})$, each elements $\widehat{\mathbf{v}}$ are the image of a vector of $\mathbb{R}^3$ by the standard isomorphism between the Lie Algebras $\mathbb{R}^3$ and $\mathfrak{so}(3)$.

$$\widehat{\mathbf{v}} = \begin{pmatrix} 0 & -v_3 & v_2 \\ v_3 & 0 & -v_1 \\ -v_2 & v_1 & 0 \end{pmatrix} \tag{2.2}$$

The twice reduced Hamiltonian of the system has the following expression (see [8]):

$$\mathscr{H}(\mathbf{z}) = \frac{|\mathbf{p}_1|^2}{2g_1} + \frac{1}{2}\Pi\mathbb{I}^{-1}\Pi - \mathbf{l}_r \cdot \mathbb{I}^{-1}\Pi + \mathscr{V}(\mathbf{u}_1) \tag{2.3}$$

where:

$$\mathscr{V}(\mathbf{u}_1) = -\int_{S_0} \frac{Gm_1 dm(\mathbf{Q})}{|\mathbf{Q} + \frac{m_1}{M_1}\mathbf{u}_1|} \tag{2.4}$$

is the potential of gravitational interaction between the gyrostat S_0 and the spherical body S_1.

The equations of the motion are given by $\dfrac{d\mathbf{z}}{dt} = \{\mathbf{z}, \mathscr{H}(\mathbf{z})\} = \mathbf{B}(\mathbf{z})\nabla_{\mathbf{z}}\mathscr{H}(\mathbf{z})$. Developing $\{\mathbf{z}, \mathscr{H}(\mathbf{z})\}$, we obtain the following group of vectorial equations of the motion:

$$\frac{d\Pi}{dt} = \Pi \times \Omega + u_1 \times \nabla_{\mathbf{u}_1}\mathscr{V}, \qquad \frac{d\mathbf{u}_1}{dt} = \frac{\mathbf{p}_1}{g_1} + \mathbf{u}_1 \times \Omega \qquad \text{and} \qquad \frac{d\mathbf{p}_1}{dt} = \mathbf{p}_1 \times \Omega - \nabla_{\mathbf{u}_1}\mathscr{V}$$

2.2 Approximate hamiltonian dynamics

We consider the multipolar development of the potential $\mathscr{V}(\mathbf{u}_1)$, supposing that the involved bodies are at much more mutual distances than the individual dimensions of the same ones. For a triaxial gyrostat the potential function, up to second harmonics, is given by the formula (see [8] for details):

$$\mathscr{V}_1 = -\frac{Gm_1}{|\mathbf{u}_1|}\left(m_0 + \frac{trace(\mathbb{I})}{2|\mathbf{u}_1|^2} - \frac{3(\mathbf{u}_1 \cdot \mathbb{I}\mathbf{u}_1)}{2|\mathbf{u}_1|^4}\right) \tag{2.5}$$

then

$$\mathscr{H}_1(\mathbf{z}) = \frac{|\mathbf{p}_1|^2}{2g_1} + \frac{1}{2}\Pi\mathbb{I}^{-1}\Pi - \mathbf{l}_r \cdot \mathbb{I}^{-1}\Pi + \mathscr{V}_1(\mathbf{u}_1) \tag{2.6}$$

If the gyrostat is close to a sphere we have:

$$\mathscr{V}_1 = -\frac{Gm_0 m_1}{|\mathbf{u}_1|} + \varepsilon\mathscr{P} \tag{2.7}$$

with ε a very small quantity and $\mathscr{P}$ is the perturbation due to the non-spherical form of the gyrostat.

We denominated as a first integrable approximation of the considered problem when $\varepsilon = 0$ and approximate dynamics to the differential equations of motion given by:

$$\frac{d\mathbf{z}}{dt} = \{\mathbf{z}, \mathscr{H}(\mathbf{z})\} = \mathbf{B}(\mathbf{z})\nabla_{\mathbf{z}}\mathscr{H}(\mathbf{z})$$

being:

$$\mathscr{H}(\mathbf{z}) = \frac{|\,\mathbf{p}_1\,|^2}{2g_1} + \frac{1}{2}\Pi\mathbb{I}^{-1}\Pi - \mathbf{l}_r \cdot \mathbb{I}^{-1}\Pi - \frac{Gm_0m_1}{|\,\mathbf{u_1}\,|} \tag{2.8}$$

2.3 Invariant manifolds of the motion

Denoting $\mathbf{u}_1 = (u_1, u_2, u_3)$, $\mathbf{p}_1 = (p_1, p_2, p_3)$ and $\Pi = (\pi_1, \pi_2, \pi_3)$, it is easy to prove that:

$$\mathbf{M}_C = \{\mathbf{z} \in \mathbb{R}^9, \pi_1 = \pi_2 = u_3 = p_3 = 0\}$$

is an invariant manifold for the flow of the equations of motion. Similar results can be obtained for the invariant manifolds $\mathbf{M}_A$, $\mathbf{M}_B$ in the cases in which the gyrostatic momentum is on the first or second axis of inertia, respectively.

As in [8], considering $\mathbf{B}(\mathbf{z})$ restricted to $\mathbf{M}_C$ and denoting this restriction as $\mathbf{B}_{\mathbf{M}_C}(\mathbf{z})$, then $\mathbf{L}_{\mathbf{M}_C} = \pi_3 + (u_1p_2 - u_2p_1)$ is a Casimir function of the Poisson tensor $\mathbf{B}_{\mathbf{M}_C}(\mathbf{z})$, and each value of the total angular momentum $\mathbf{L}_{\mathbf{M}_C} = \mathbf{L}$ constant, the dynamics on the fiber $\mathbf{M}_C \cap (\mathbf{L}_{\mathbf{M}_C} = \mathbf{L})$ adopts canonical form.

Making an adequate canonical transformation, the Hamiltonian is:

$$\mathscr{H} = \frac{|\,\mathbf{P}_1\,|^2}{2} + \alpha(\beta - (xP_2 - yP_1))^2 - \frac{1}{|\,\mathbf{x}\,|} \tag{2.9}$$

with $\alpha = \dfrac{\sigma}{2C}$, $\beta = \dfrac{L-l}{\sigma^2}$, $\sigma = \mu(1-\mu)$ and $\mu = m_0$ describes the planar dynamics of a gyrostat in Newtonian interaction with a spherical rigid body on the fiber $\mathbf{M}_C \cap (\mathbf{L}_{\mathbf{M}_C} = \mathbf{L})$ of the invariant manifold $\mathbf{M}_C$.

In which it follows we will consider the Hamiltonian in polar symplectics coordinates:

$$\mathscr{H} = \frac{1}{2}\left(p_r^2 + \frac{p_\theta^2}{r^2}\right) + \alpha(\beta - p_\theta)^2 - \frac{1}{r} \tag{2.10}$$

3 Qualitative study of the Hamiltonian flow

In this section we study the topology of the invariant manifolds $\mathscr{H}^{-1}(h) = E_h$ and I_{hk}. To give the topological classification of these invariant sets we need some notation and some new results.

Note that $z_e = (r_e, \theta_e, p_{r_e}, p_{\theta_e}) \in \mathbf{E}$ is an equilibrium point of the Hamiltonian flow if and only if $\tilde{z}_e = (r_e, \theta_e)$ is a critical point of the amended potential. Moreover, $\pi(z_e) = \tilde{z}_e$, where $\pi : \mathbf{E} \longrightarrow \mathbb{R}^+ \times S^1$ is the natural projection. For this reason, when $27\alpha\beta^4 - 128 > 0$, the Hamiltonian has two families of equilibrium points; one family of equilibrium points when $27\alpha\beta^4 - 128 = 0$ and the Hamiltonian does not have equilibria when $27\alpha\beta^4 - 128 < 0$. We denote by $h_i = \mathscr{H}(r_i, \theta_i, 0, p_{\theta_i})$ $(i = 1,2,3)$, the values of the Hamiltonian $\mathscr{H}$ at its equilibrium points and c_j, $(j = 1,2,3,4)$ the extremes of the energy surface $\mathscr{H}^{-1}(h)/S^1$.

To classify the trajectories we need the equilibrium points $h_i\,(i = 1,2,3)$, the values $c_j\,(j = 1,2,3,4)$ and some new values a_1 and a_2. These last values are the real roots respect to k of the equation $h - \alpha\,(\beta - k)^2 = 0$. Is easy to see that, between a_1 and a_2, all the trajectories are not bounded . When we are in $k = 0$ the orbits are not bounded too. In the rest of the cases we have not energy surface, a point or a bounded trajectory.

Finally, let S^{n-1} be the sphere in $\mathbb{R}^n$, with $n > 1$ and Y the union of two open solid tori identifying point to point the points of two circles of each torus which cannot be contracted to a single point inside the corresponding torus (see [4] for details).

3.1 Energy surfaces

In this subsection we can observe the figures that represent the energy surfaces.

First case: $27\alpha\beta^4 - 128 > 0$.

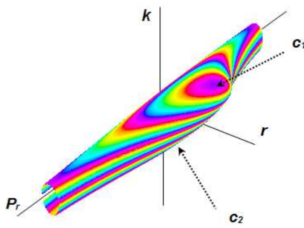

Figure 1: $\mathscr{H}^{-1}(h)/S^1$ for $27\alpha\beta^4 - 128 > 0$ and $h < h_2$, where $k = p_\theta$ and c_1, c_2 the extremes.

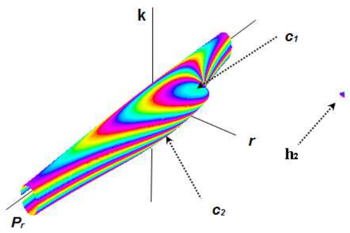

Figure 2: $\mathscr{H}^{-1}(h)/S^1$ for $27\alpha\beta^4 - 128 > 0$ and $h = h_2$, where $k = p_\theta$, h_2 the equili brium point and c_1, c_2 the extremes.

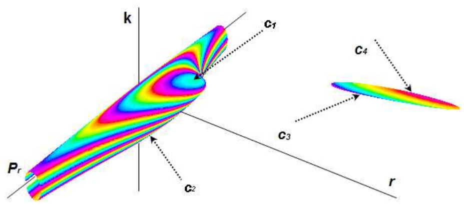

Figure 3: $\mathscr{H}^{-1}(h)/S^1$ for $27\alpha\beta^4 - 128 > 0$ and $h_2 < h < 0$, where $k = p_\theta$ and c_1, c_2, c_3, c_4 the extremes.

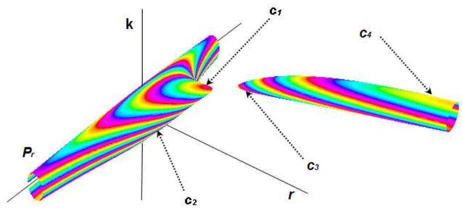

Figure 4: $\mathscr{H}^{-1}(h)/S^1$ for $27\alpha\beta^4 - 128 > 0$ and $0 < h < h_1$, where $k = p_\theta$ and c_1, c_2, c_3, c_4 the extremes.

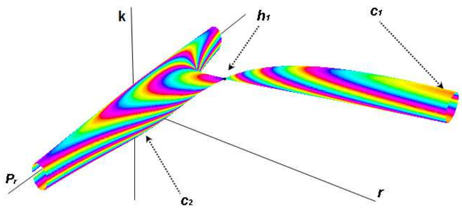

Figure 5: $\mathscr{H}^{-1}(h)/S^1$ for $27\alpha\beta^4 - 128 > 0$ and $h = h_1$, where $k = p_\theta$, h_1 the equili brium point and c_1, c_2 the extremes.

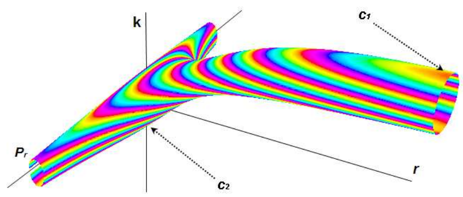

Figure 6: $\mathscr{H}^{-1}(h)/S^1$ for $27\alpha\beta^4 - 128 > 0$ and $h > h_1$, where $k = p_\theta$ and c_1, c_2 the extremes.

Second case: $27\alpha\beta^4 - 128 = 0$.

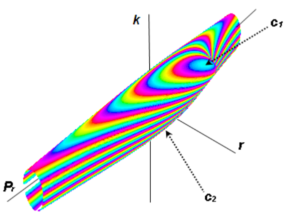

Figure 7: $\mathscr{H}^{-1}(h)/S^1$ for $27\alpha\beta^4 - 128 = 0$ and $h < h_3$, where $k = p_\theta$ and c_1, c_2 the extremes.

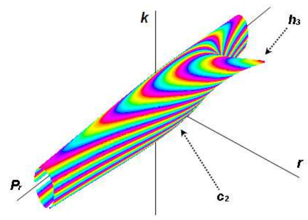

Figure 8: $\mathscr{H}^{-1}(h)/S^1$ for $27\alpha\beta^4 - 128 = 0$ and $h = h_3$, where $k = p_\theta$, h_3 the equili brium point and c_1, c_2 the extremes.

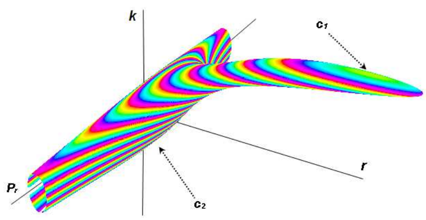

Figure 9: $\mathscr{H}^{-1}(h)/S^1$ for $27\alpha\beta^4 - 128 = 0$ and $h_3 < h < 0$, where $k = p_\theta$ and c_1, c_2 the extremes.

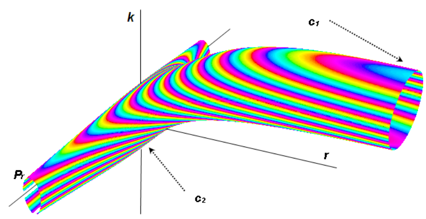

Figure 10: $\mathscr{H}^{-1}(h)/S^1$ for $27\alpha\beta^4 - 128 = 0$ and $h \geq 0$, where $k = p_\theta$ and c_1, c_2 the extremes.

Third case: $27\alpha\beta^4 - 128 < 0$.

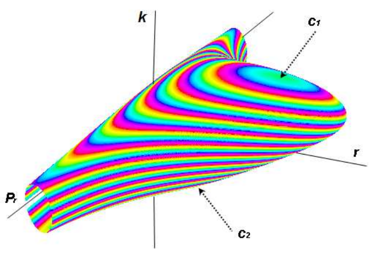

Figure 11: $\mathscr{H}^{-1}(h)/S^1$ for $27\alpha\beta^4 - 128 < 0$ and $h < 0$, where $k = p_\theta$ and c_1, c_2 the extremes.

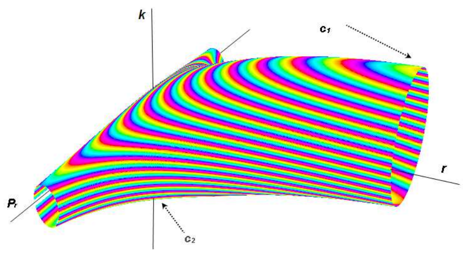

Figure 12: $\mathscr{H}^{-1}(h)/S^1$ for $27\alpha\beta^4 - 128 < 0$ and $h \geq 0$, where $k = p_\theta$ and c_1, c_2 the extremes.

The different colors in the pictures represent the contour line of the energy surfaces for constant angular momentum and this allow us to see more easily if the trajectories are bounded.

3.2 Topology of the invariant manifolds

In the following tables we describe the topological classification of I_h and I_{hk}.

h	I_h	I_{hk}
$h < h_2$	$\{S^3\backslash S^1\}$, See Fig. 1	$S^1\times S^1$, $c_2<k<0$ $S^1\times\mathbb{R}$, $k=0$ $S^1\times S^1$, $0<k<c_1$
$h=h_2$	$\{S^3\backslash S^1\}\cup\{S^1\}$, See Fig. 2	$S^1\times S^1$, $c_2<k<0$ $S^1\times\mathbb{R}$, $k=0$ $S^1\times S^1$, $0<k<c_1$ $S^1\times S^1$, $k=h_2$
$h_2<h<0$	$\{S^3\backslash S^1\}\cup\{S^3\}$, See Fig. 3	$S^1\times S^1$, $c_2<k<0$ $S^1\times\mathbb{R}$, $k=0$ $S^1\times S^1$, $0<k<c_1$ $S^1\times S^1$, $c_3<k<c_4$
$0<h<h_1$	$\{S^3\backslash S^1\}\cup\{S^3\backslash S^1\}$, See Fig. 4	$S^1\times S^1$, $c_2<k<0$ $S^1\times\mathbb{R}$, $k=0$ $S^1\times S^1$, $0<k<c_1$ $S^1\times S^1$, $c_3<k<a_1$ $S^1\times\mathbb{R}$, $a_1<k<a_2$ $S^1\times S^1$, $a_2<k<c_4$
$h=h_1$	Y, See Fig. 5	$S^1\times S^1$, $c_2<k<0$ $S^1\times\mathbb{R}$, $k=0$ $S^1\times S^1$, $0<k<a_1$ $S^1\times\mathbb{R}$, $a_1<k<a_2$ $S^1\times S^1$, $a_2<k<c_1$
$h>h_1$	$S^3\backslash\{S^1\cup S^1\}$, See Fig. 6	$S^1\times S^1$, $c_2<k<0$ $S^1\times\mathbb{R}$, $k=0$ $S^1\times S^1$, $0<k<c_1$ $S^1\times S^1$, $0<k<a_1$ $S^1\times\mathbb{R}$, $a_1<k<a_2$ $S^1\times S^1$, $a_2<k<c_1$

Table 1: Topological classification of I_h and I_{hk} when $27\alpha\beta^4-128>0$.

h	I_h	I_{hk}
$h<h_3$	$S^3\backslash S^1$, See Fig. 7	$S^1\times S^1$, $c_2<k<0$ $S^1\times\mathbb{R}$, $k=0$ $S^1\times S^1$, $0<k<c_1$
$h=h_3$	$S^3\backslash S^1$, See Fig. 8	$S^1\times S^1$, $c_2<k<0$ $S^1\times\mathbb{R}$, $k=0$ $S^1\times S^1$, $0<k<c_1$
$h_3<h<0$	$S^3\backslash S^1$, See Fig. 9	$S^1\times S^1$, $c_2<k<0$ $S^1\times\mathbb{R}$, $k=0$ $S^1\times S^1$, $0<k<c_1$
$h\geq 0$	$S^3\backslash\{S^1\cup S^1\}$, See Fig. 10	$S^1\times S^1$, $c_2<k<0$ $S^1\times\mathbb{R}$, $k=0$ $S^1\times S^1$, $0<k<a_1$ $S^1\times\mathbb{R}$, $a_1<k<a_2$ $S^1\times S^1$, $a_2<k<c_1$

Table 2: Topological classification of I_h and I_{hk} when $27\alpha\beta^4-128=0$.

h	I_h	I_{hk}
$h<0$	$S^3\backslash S^1$, See Fig. 11	$S^1\times S^1$, $c_2<k<0$ $S^1\times\mathbb{R}$, $k=0$ $S^1\times S^1$, $0<k<c_1$
$h\geq 0$	$S^3\backslash\{S^1\cup S^1\}$, See Fig. 12	$S^1\times S^1$, $c_2<k<0$ $S^1\times\mathbb{R}$, $k=0$ $S^1\times S^1$, $0<k<a_1$ $S^1\times\mathbb{R}$, $a_1<k<a_2$ $S^1\times S^1$, $a_2<k<c_1$

Table 3: Topological classification of I_h and I_{hk} when $27\alpha\beta^4-128<0$.

4 Action-angle variables

In this section we calculate, by means of the Hamilton-Jacobi Theory, the action-angle variables and the expression of the Hamiltonian in these variables. These variables are useful to calculate the modified Keplerian elements and the planetary equations that are derived of these elements.

The action-angle variables can be defined by:

$$J_\theta = \frac{1}{2\pi}\int_0^{2\pi} p_\theta d\theta = k \tag{4.1}$$

$$J_r = \frac{1}{2\pi}\int_{r_1}^{r_2} \sqrt{2h - 2\widetilde{\mathscr{V}}(r) - \frac{1+2\alpha r^2}{r^2}\left(k - \frac{2\alpha\beta r^2}{1+2\alpha r^2}\right)^2} dr \tag{4.2}$$

where:

$$\widetilde{\mathscr{V}}(r) = \frac{\alpha\beta^2}{1+2\alpha r^2} - \frac{1}{r}$$

is the expression of the amended potential in polar-symplectic coordinates.

In order to calculate J_r we use the Cauchy Residue theorem. The expressions for J_θ and J_r are:

$$J_\theta = k \tag{4.3}$$

$$J_r = -J_\theta - \frac{1}{\sqrt{2\left(\alpha\beta^2 - h - 2\alpha\beta J_\theta + \alpha J_\theta^2\right)}} \tag{4.4}$$

The transformation from polar-symplectic variables to action-angle variables can be defined in the region where the following equation in r:

$$2h - 2\widetilde{\mathscr{V}}(r) - \frac{1+2\alpha r^2}{r^2}\left(k - \frac{2\alpha\beta r^2}{1+2\alpha r^2}\right)^2 = 0 \tag{4.5}$$

has two different real roots, according to the parameters α, β and h.

By means of Sturm Algorithm we obtain the region where (4.5) has two different real roots. This region is given by the following inequalities:

$$\frac{1}{2\left(h - \alpha(\beta - k)^2\right)} + k^2 < 0 \tag{4.6}$$

$$h - \alpha(\beta - k)^2 < 0 \tag{4.7}$$

In the next figure the region defined by the inequalities (4.6) and (4.7) is presented

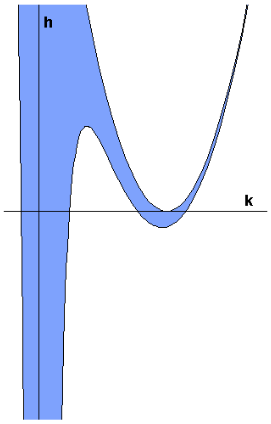

Figure 13: Region where (4.5) has two different real roots

Solving h in (4.4) we have the Hamiltonian expressed by means of these new variables:

$$\mathscr{H} = -\frac{1}{2\left(J_r + J_\theta\right)^2} + \alpha\left(\beta - J_\theta\right)^2 \tag{4.8}$$

5 Delaunay variables

Using the next transformations to Delaunay variables:

$$G = J_\theta, \quad L = J_r + J_\theta$$

the Hamiltonian $\mathscr{H}$ takes the form:

$$\mathscr{H} = -\frac{1}{2L^2} + \alpha\left(\beta - G\right)^2 \tag{5.1}$$

In Delaunay variables, the inequalities (4.6) and (4.7) become to:

$$G^2 - L^2 < 0 \tag{5.2}$$

$$-\frac{1}{2L^2} < 0 \tag{5.3}$$

And the region defined by the previous inequalities is:

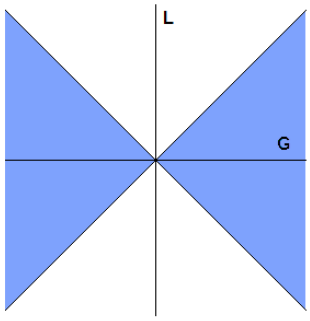

Figure 14: Region for Delaunay variables

6 Planetary Equations

Using the Classical Perturbation Theory, we obtain the modified Keplerian elements, denoted by (a,e,l,g).

- a is the semi-major axis and its expression is:

$$a = \frac{-1}{2\left(h-\alpha\,(\beta-k)^2\right)} \tag{6.1}$$

- e is the eccentricity:

$$e = \left(1+2\left(h-\alpha\,(\beta-k)^2\right)k^2\right)^{\frac{1}{2}} \tag{6.2}$$

- l is the mean anomaly:

$$l = t - n^{-1}(E - e\sin E) \tag{6.3}$$

  where t is the time, $n = a^{-\frac{3}{2}}$ and E is the eccentric anomaly.

- g is the argument of perihelion:

$$g = \theta - f - 2\alpha\,(t-l)\left(a^{\frac{1}{2}}\left(1-e^2\right)^{\frac{1}{2}} - \beta\right) \tag{6.4}$$

  where f is the true anomaly.

It can be proved that the planetary equations are the same as the Kepler problem but the perturbation theory for this system is more complicated because the Perturbed Kepler Problem has:

$$\theta = g + f$$

and for our Hamiltonian we have:

$$\theta = g + f + 2\alpha\,(t-l)\left(a^{\frac{1}{2}}\left(1-e^2\right)^{\frac{1}{2}} - \beta\right)$$

For more details about the planetary equations of Kepler problem see [2].

7 Conclusions

In this paper we have considered a first integrable approximation of a roto-translatory problem. We have described the Hamiltonian dynamics on the fibers of constant value of the total angular momentum $(\mathbf{L}_{\mathbf{M}_C} = \mathbf{L})$ in the invariant manifold $\mathbf{M}_C$. A complete topological classification of the invariant sets I_h, I_k and I_{hk} is given by means of Liouville-Arnold theorem and some specifics techniques. The action-angle variables have been obtained and the region of the phase space where they can be defined. We have calculated the Delaunay variables and the modified Keplerian elements of this problem useful to elaborate a perturbation theory. The results of this work have a direct application to the study of two body roto-translatory problems where the rotation of one of them influences strongly in the orbital motion of the system. In particular, we can apply these results to binary asteroids.

Acknowledgments. The authors thanks Professor A. Vigueras for this comments and suggestions during the revision of this manuscript. Likewise, the authors acknowledge the fruitful comments from the anonymous reviewer.

This project is made possible by a grant from the Consejería de Educación y Cultura de la Comunidad Autónoma de la Región de Murcia (Spain) (Ayudas Individualizadas de Formación del Profesorado).

References

[1] V I Arnold, V V Kozlov and A I Neishtadt, Dynamical Systems III (Encyclopaedia of Mathematical Sciences), *Springer Verlag*, Berlin (1978).

[2] H Goldstein, Mecnica clsica, *Editorial Revert*, Barcelona (1988).

[3] E Leimanis, The general problem of the motion of coupled rigid bodies about a fixed point, *Springer Verlag*, Berlin (1965).

[4] J Llibre, A E Teruel, C Valls and A de la Fuente, Phase portraits of the two-body problem with Manev potential, *Journal of Physics A: Mathematical and General* **34**, (2001) 1919–1934.

[5] V V Rumiantsev, On the stability of stationary motions of rigid bodies with cavities containing fluid, *J. Appl. Math. Mech.*. **26**, (1962), 1485–1505.

[6] J A Vera, Reducciones, equilibrios y estabilidad en dinámica de sólidos rígidos y giróstatos, Tesis Doctoral, Universidad Politécnica de Cartagena (2004).

[7] J A Vera and A Vigueras, Libration points of a gyrostat in a generalized three body problem, *Advances in the Astronautical Sciences*, **123**, (2005) 2775–2795.

[8] J A Vera and A Vigueras, Hamiltonian dynamics of a gyrostat in the n-body problem: relative equilibria. *Celestial Mechanics and Dynamical Astronomy*, **94** (3), (2006) 289–315.

[9] V Volterra, *Acta Mathematica*, **22** (201), (1899).